Root anatomy and biomechanical properties: improving predictions through root cortical and stele properties - Supplementary material

G. J. Meijer* J. P. Lynch† J. G. Chimungu‡ K. W. Loades§

Contents

1 Introduction **2**

2 Root geometry and anatomy **2**

3 Constitutive equations — biomechanics **3**

4 Compatibility equations **3**

5 Equilibrium equations **4**

6 Elastic behaviour **4**

7 Root yielding — initial cortex failure **5**

8 Hardening behaviour of roots **6**
8.1 Behaviour of a single root segment 6
8.2 Cortex failure as a discrete process 10
8.3 Cortex failure as a continuous process 11
8.4 Stele–cortex interface debonding 12

9 Nondimensionalised solutions **15**
9.1 Nondimensional parameter groups 15
9.2 Dimensionless stress–strain equations 16

10 Fitting of tensile stress–strain curves and determination of the yield point **17**

*Department of Architecture and Civil Engineering, University of Bath, Bath BA2 7AY, UK. ORCID: 0000-0002-2815-5480. Corresponding author: gjm36@bath.ac.uk

†Department of Plant Science, The Pennsylvania State University, University Park, PA 16802, USA. ORCID: 0000-0002-7265-9790

‡Department of Soil and Crop Sciences, Lilongwe University of Agriculture and Natural Resources, Lilongwe, Malawi. ORCID: 0000-0002-0330-0872

§Ecological Sciences, The James Hutton Institute, Dundee DD2 5DA, UK. ORCID: 0000-0003-2415-3549

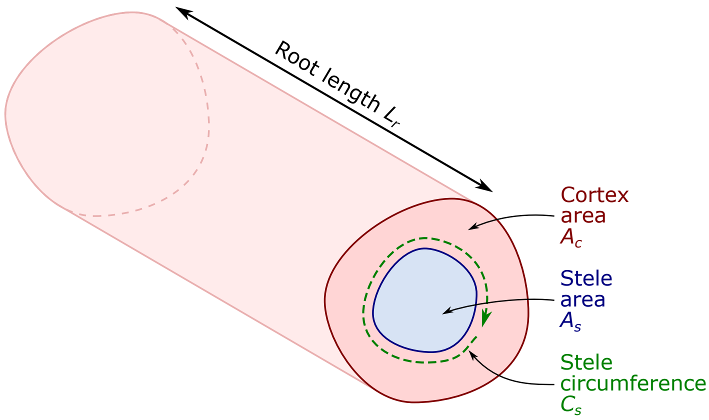

Figure 1: Graphical depiction of root geometry

11 Symbols **19**
11.1 Parameter and subscript logic 20
11.2 Full list of symbols 22

1 Introduction

This document contains supplementary information for to the manuscript "Root anatomy and biomechanical properties: improving predictions through root cortical and stele properties". It details all assumptions and mathematical derivations of the proposed closed-form analytical solution for the full stress–strain behaviour of plant roots in full detail (Sections 2–9). In addition, it provides additional detail about the methodology used for fitting root elongation–root tensile force data as measured during a tensile test on single roots (Section 10).

All parameters in this manuscript (in square brackets) are expressed in general dimensions unless otherwise specified, using [F] for units of force, [L] for units of length and [-] for dimensionless parameters. A full list of symbols is provided in Section 11.

2 Root geometry and anatomy

Roots are assumed as prisms[1] with a constant cross-sectional area A_r [L^2] along its axis. The root has a length L_r [L]. The root contains a prismatic-shapes stele with a constant cross-sectional area A_s [L^2] and circumference C_s [L] along the length axis. The cortex — the outer layer of the root — has a cross-sectional area $A_c = A_r - A_s$ (Figure 1). The root and stele do not necessarily have to be circular in shape. The stele–cortex interface is assumed to be an infinitesimally thin layer between the cortex and stele. The total cross sectional area of the interface is therefore $C_s L_r$ [L^2].

The axial displacement of (any point along the) stele and cortex is indicated by u_s [L] and u_c [L], which may vary along root axis s [L].

[1]Three-dimensional shapes created by extruding a two-dimensional polygon in the direction normal to the plane of the polygon. The shape and area cross-section will therefore be constant along the extruded dimension

3 Constitutive equations — biomechanics

The behaviour of the stele and cortex is assumed as linear elastic until failure. The stele and the cortex can individually sustain a maximum tensile force, $T_{s,u}$ [F] and $T_{c,u}$ [F] respectively, equal to:

$$T_{s,u} = A_s t_{s,u} = E_s A_s \epsilon_{s,u} \tag{1}$$

$$T_{c,u} = A_c t_{c,u} = E_c A_c \epsilon_{c,u} \tag{2}$$

where $t_{s,u}$ and $t_{c,u}$ are the tensile strength [FL^{-2}], $\epsilon_{s,u}$ and $\epsilon_{c,u}$ the tensile strain to failure [LL^{-1}], and $E_s = t_{s,u}/\epsilon_{s,u}$ and $E_c = t_{c,u}/\epsilon_{c,u}$ the linear elastic Young's moduli for the stele and cortex respectively [FL^{-2}]. Failure in both the stele and the cortex is assumed to be brittle, i.e. once the stress exceeds the strength the stress is immediately reduced to zero and all strength is lost.

Observations during root tensile testing have shown that the cortex often starts cracking/breaking before the root eventually fails, often in multiple places along the root axis. This suggests that the cortex breaks at smaller levels of strain compared to the stele, i.e. $\epsilon_{c,u} < \epsilon_{s,u}$.

Interface shear resistance may mobilise in the interface between cortex and stele. The shear force T_i [FL^{-1}, i.e. in shear force per unit length of root] transferred between the two is assumed to be linear elastic and proportional with the differential displacement in the stele (u_s) and cortex (u_c) on either side of the interface:

$$T_i = C_s t_i \tag{3}$$

$$t_i = k_i u_i \tag{4}$$

$$u_i = u_s - u_c \tag{5}$$

where t_i [FL^{-2}] is the currently mobilised interface shear stress and k_i [FL^{-3}] is the linear elastic interface stiffness coefficient, defined as:

$$k_i = \frac{t_{i,u}}{u_{i,u}} \tag{6}$$

where $t_{i,u}$ [FL^{-2}] and $u_{i,u}$ [L] are the stress and difference in stele and cortex displacement u_i at which the interface will fail/debond. Interface failure is assumed as brittle, i.e. when the interface strength is exceeded, the interface immediately loses all strength and the stele and cortex can freely slide along each other. The maximum shear force the interface can sustain before debonding occurs ($T_{i,u}$, per unit length of interface) equals:

$$T_{i,u} = C_s k_i u_{i,u} \tag{7}$$

4 Compatibility equations

All strains are defined in terms of engineering strains, i.e. strains are equal to the elongation divided by the original length of the element.

During a tensile tests, the root is subjected to axial elongation u_r [L]. This results in an average strain along the root ϵ_r [LL^{-1}]:

$$\epsilon_r = u_r / L_r \tag{8}$$

This is an *average* measure for strain along the root since it is calculated using the total root elongation (different in displacement between the two root ends) and the root length.

The strains in the stele and cortex at any point along the root satisfy:

$$\epsilon_s = \frac{\mathrm{d}u_s}{\mathrm{d}s} \tag{9}$$

$$\epsilon_c = \frac{\mathrm{d}u_c}{\mathrm{d}s} \tag{10}$$

where u_s and u_c are the axial displacements of the stele and the cortex at axial position s [L] along the root respectively.

5 Equilibrium equations

Static equilibrium of forces is assumed throughout the entire root, so any dynamic forces — associated with acceleration of masses — are not considered. The tensile force T_r [F] must be constant along the entire root and is equal to the sum of forces carried by the stele T_s [F] and the cortex T_c [F] at any point along the root, see Figure 2:

$$T_r = T_s + T_c \tag{11}$$

Mobilisation of stele–cortex interface resistance may however change how the root force T_r is distributed across the stele and cortex. Equilibrium of forces along a infinitesimal section of stele and cortex (length $\mathrm{d}s$) must satisfy (see Figure 2):

$$\frac{\mathrm{d}T_s}{\mathrm{d}s} = T_i \qquad \frac{\mathrm{d}T_c}{\mathrm{d}s} = -T_i \tag{12}$$

With the assumed geometry, the compatibility relationships and the (linear elastic) constitutive behaviour, these two differential equations can alternatively be expressed in terms of stele and cortex displacements u_s and u_c, see Figure 2.

$$\frac{\mathrm{d}T_s}{\mathrm{d}s} = E_s A_s \frac{\mathrm{d}\epsilon_s}{\mathrm{d}s} = E_s A_s \frac{\mathrm{d}^2 u_s}{\mathrm{d}s^2} = C_s k_i (u_s - u_c) \tag{13}$$

$$\frac{\mathrm{d}T_c}{\mathrm{d}s} = E_c A_c \frac{\mathrm{d}\epsilon_c}{\mathrm{d}s} = E_c A_c \frac{\mathrm{d}^2 u_c}{\mathrm{d}s^2} = -C_s k_i (u_s - u_c) \tag{14}$$

The stress–strain response of both the stele and cortex along root axis s can be found by solving this set of second order differential equations in terms of stele and cortex displacements u_s and u_c.

These solutions must satisfy the boundary conditions of the problem, e.g. the conditions at the clamps and at any locations of cortex, stele or interface breakages.

6 Elastic behaviour

At the start of each tensile test, the stele, cortex and interface are all fully intact. The boundary conditions for the equilibrium equations at the fixed clamp ($s = 0$) are $u_s = u_c = 0$, while at the displacing clamp ($s = L_r$), $u_s = u_c = u_r$.

The solution to Equations 13 and 14 that satisfies these boundary conditions is:

$$u_s = u_c = \frac{u_r}{L_r} s = \epsilon_r s \tag{15}$$

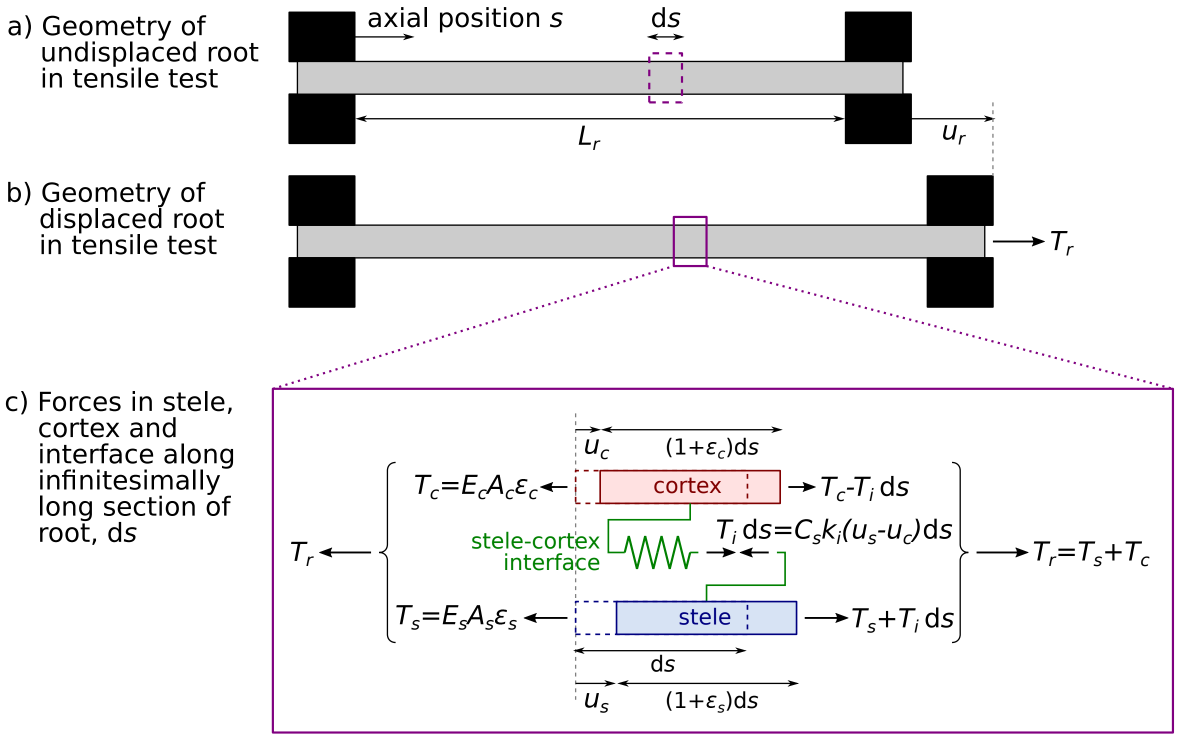

Figure 2: Schematisation of root elongation in tension test, and mechanical model of forces in stele, cortex and interface along an infinitesimal section of root ds.

Therefore:

$$T_s = E_s A_s \epsilon_r \qquad T_c = E_c A_c \epsilon_r \tag{16}$$

and therefore the root tensile force T_r is given by:

$$T_r = (E_s A_s + E_c A_c)\epsilon_r \tag{17}$$

7 Root yielding — initial cortex failure

Observations by the authors during prior tensile tests (e.g. Chimungu et al., 2015) showed that the cortex often ruptures and cracks at elongations much smaller than elongations required to fail the entire root. This observation forms the basis of the model development. Cortex failure will result in a permanent reduction in root tangent stiffness as the root is now irreparably damaged. This point of a marked change in root tensile behaviour is associated with the yield point of the root stress–strain curve (characterised by yield stress $t_{r,y}$ and yield strain $\epsilon_{r,y}$).

At the point of initial cortex breakage, which may happen at any point along the root, the strains $\epsilon_r = \epsilon_{r,y} = \epsilon_{c,u}$. Using Equation 17, the yield force $T_{r,y}$ is given by:

$$T_{r,y} = A_r t_{r,y} = (E_s A_s + E_c A_c)\epsilon_{c,u} \tag{18}$$

At the location where the cortex broke it can no longer transfer any axial force. This means the stele must carry the full tensile force T_r at the location of the cortex breakage. This will only be possible when the stele is strong enough to carry the entire yield force without breaking, i.e. when:

$$T_{r,y} < T_{s,u} \tag{19}$$

If this condition does not hold, the stele will break simultaneously with or shortly after the initial cortex failure and the entire root will be broken. Such a reduction in strength after yielding is known as 'softening' material behaviour. The yield strength $t_{r,y}$ of a softening root will be equal to the maximum root strength $t_{r,u}$. In the authors' experience most roots instead demonstrate 'hardening' behaviour, which means the root stresses can increase beyond the root yield strength. This behaviour will be the focus of the remainder of this study.

8 Hardening behaviour of roots

8.1 Behaviour of a single root segment

When Equation 19 holds, the root will be able to carry stresses exceeding the yield stress before breaking ('hardening' behaviour).

Assume the cortex breaks at location $s = L_1$. Equilibrium Equations 13 and 14 can be solved seperately for the root segments on either side of the cortex breakage (domains $0 \leq s \leq L_1$ and $L_1 \leq s \leq L_r$). Additional boundary conditions — in addition to the already defined boundary conditions at the clamps — are required at the location where the two segments connect:

- Stresses and strains in the cortex must be zero on either sides of the stele breakage, since the cortex cannot carry any stress across the crack: $\epsilon_c^+ = \epsilon_c^- = 0$ ($^+$ and $^-$ indicate the position on either side of the cortex breakage)
- The stele remains connected: $u_s^+ = u_s^-$ and $\epsilon_s^+ = \epsilon_s^-$
- The cortex is disconnected across the break (so $u_c^+ \neq u_c^-$)

Any root with cortex breakages in one of more locations can be seen as consisting of a number of 'segments', each with a (potentially different) length L_b (Figure 3b). At one end of the segment (say $s = 0$) the displacements in cortex and stele are equal ($u_s = u_c$). This may be the case at a clamp, but also halfway between two neighbouring cortex breakages because of symmetry. At the other end of the segment (say $s = L_b$) the cortex is broken.

Let us now analyse the behaviour of a single 'segment'. At the start of the segment ($s = 0$), $u_s = u_c = u_1$ where u_1 is a known displacement. At the end of a segment ($s = L_b$) the cortex is broken ($t_c = \epsilon_c = 0$) and $u_s = u_2$ where u_2 is a known displacement, see Figure 3a. The total elongation u_b [L] of the segment is therefore:

$$u_b = u_2 - u_1 \tag{20}$$

Let us for now assume that the stele–cortex interface in the region $0 \leq s \leq L_b$ is strong enough to remain fully intact along the entire length of the segment (we will revisit this assumption later in Section 8.4).

Differentiating the equation for interface displacement (Equation 5) twice with respect to position s gives:

$$\frac{\mathrm{d}^2 u_i}{\mathrm{d}s^2} = \frac{\mathrm{d}^2 u_s}{\mathrm{d}s^2} - \frac{\mathrm{d}^2 u_c}{\mathrm{d}s^2} \tag{21}$$

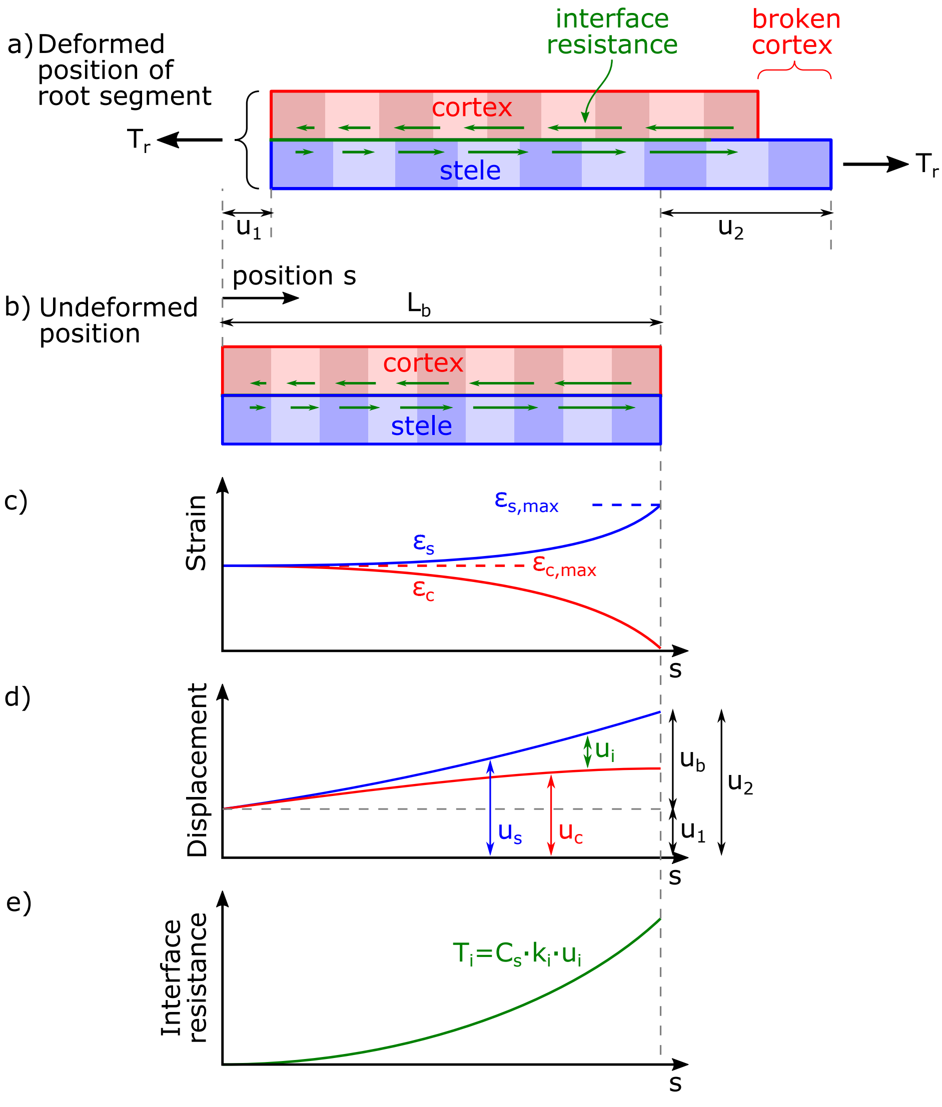

Figure 3: Schematic of root strains and displacements along the root axis of a segment of root (with no debonding of the stele–cortex interface).

Now substitute equilibrium Equations 13 and 14 into Equation 21:

$$\frac{\mathrm{d}^2 u_i}{\mathrm{d}s^2} = \zeta^2 u_i \tag{22}$$

where:

$$\zeta = \sqrt{\beta_s + \beta_c} \tag{23}$$

$$\beta_s = \frac{C_s k_i}{E_s A_s} \tag{24}$$

$$\beta_c = \frac{C_s k_i}{E_c A_c} \tag{25}$$

Solving this second order differential equation (Equation 22) for u_i gives :

$$u_i = u_s - u_c = c_1 \exp(\zeta s) + c_2 \exp(-\zeta s) \tag{26}$$

Expressions for u_s and u_c can now by found through double integration of Equations 13 and 14 and substituting the derived expression for u_i (Equation 26). This gives:

$$u_s = \frac{\beta_s}{\zeta^2}[c_1 \exp(\zeta s) + c_2 \exp(-\zeta s)] + c_3 s + c_4 \tag{27}$$

$$u_c = -\frac{\beta_c}{\zeta^2}[c_1 \exp(\zeta s) + c_2 \exp(-\zeta s)] + c_3 s + c_4 \tag{28}$$

Boundary conditions are required to solve for the unknown integration coefficients c_1, c_2, c_3 and c_4. At $s = 0$, the cortex and stele displacements are known, so:

$$u_s(s = 0) = u_1 \tag{29}$$

$$u_c(s = 0) = u_1 \tag{30}$$

At $s = L_b$, the cortex is broken (so the stress in the cortex must be zero, as it cannot carry any stress across the breakage) and the elongation of the stele must be equal to the known deformation applied to this segment of root:

$$t_c(s = L_b) = \epsilon_c(s = L_b) = \frac{\partial u_c(s = L_b)}{\partial s} = 0 \tag{31}$$

$$u_s(s = L_b) = u_2 \tag{32}$$

Using these boundary to solve for the constants c_1, c_2, c_3 and c_4 gives:

$$c_1 = \frac{u_b \zeta^2}{2\beta_s \sinh(\zeta L_b) + 2\beta_c \zeta L_b \cosh(\zeta L_b)} \tag{33}$$

$$c_2 = -c_1 \tag{34}$$

$$c_3 = \frac{\beta_c \zeta u_b \cosh(\zeta L_b)}{\beta_s \sinh(\zeta L_b) + \beta_c \zeta L_b \cosh(\zeta L_b)} \tag{35}$$

$$c_4 = u_1 \tag{36}$$

Stele deformations u_s and cortex deformations u_c, as function of position s along the segment ($0 \leq s \leq L_b$), are therefore (Figure 3d):

$$u_s = u_1 + u_b \left[\frac{\beta_c \zeta \cosh(\zeta L_b) s + \beta_s \sinh(\zeta s)}{\beta_c \zeta L_b \cosh(\zeta L_b) + \beta_s \sinh(\zeta L_b)} \right] \tag{37}$$

$$u_c = u_1 + u_b \left[\frac{\beta_c \zeta \cosh(\zeta L_b) s - \beta_c \sinh(\zeta s)}{\beta_c \zeta L_b \cosh(\zeta L_b) + \beta_s \sinh(\zeta L_b)} \right] \tag{38}$$

And so the relative interface displacement u_i as function of position s (Figure 3d,e):

$$u_i = u_s - u_c = u_b \left[\frac{\zeta^2 \sinh(\zeta s)}{\beta_c \zeta L_b \cosh(\zeta L_b) + \beta_s \sinh(\zeta L_b)} \right] \tag{39}$$

The strains along the stele and the cortex, as function of position s, can be found by differentiating the displacements u_s and u_c with respect to position s (Figure 3c):

$$\epsilon_s = \frac{\mathrm{d}u_s}{\mathrm{d}s} = \frac{u_b}{L_b} \left[\frac{\beta_c \zeta L_b \cosh(\zeta L_b) + \beta_s \zeta L_b \cosh(\zeta s)}{\beta_c \zeta L_b \cosh(\zeta L_b) + \beta_s \sinh(\zeta L_b)} \right] \tag{40}$$

$$\epsilon_c = \frac{\mathrm{d}u_c}{\mathrm{d}s} = \frac{u_b}{L_b} \left[\frac{\beta_c \zeta L_b \cosh(\zeta L_b) - \beta_c \zeta L_b \cosh(\zeta s)}{\beta_c \zeta L_b \cosh(\zeta L_b) + \beta_s \sinh(\zeta L_b)} \right] \tag{41}$$

This shows that, as a result of cortex breakage, the strains in the cortex and stele will not be constant along the root axis, but vary as function of position s. Stele stresses and strains will be larger near the cortex breakage, while cortex stresses and strains will be smaller nearer the cortex breakage, see Figure 3c.

The largest strain in the stele ($\epsilon_{s,max}$) can be obtained by finding the largest value of ϵ_s (Equation 40) along the segment domain $0 \leq s \leq L_b$. The largest value occurs at $s = L_b$, see Figure 3c:

$$\epsilon_{s,max} = \frac{u_b}{L_b} \left[\frac{\zeta^3 L_b \cosh(\zeta L_b)}{\beta_c \zeta L_b \cosh(\zeta L_b) + \beta_s \sinh(\zeta L_b)} \right] \tag{42}$$

The largest strain in the cortex ($\epsilon_{c,max}$) can be obtained by finding the largest value of ϵ_c (Equation 41) along the segment domain $0 \leq s \leq L_b$. The largest value occurs at $s = 0$, see Figure 3c:

$$\epsilon_{c,max} = \frac{u_b}{L_b} \left[\frac{\beta_c \zeta L_b (\cosh(\zeta L_b) - 1)}{\beta_c \zeta L_b \cosh(\zeta L_b) + \beta_s \sinh(\zeta L_b)} \right] \tag{43}$$

The largest interface relative displacement ($u_{i,max}$) can be obtained by finding the largest value of u_i (Equation 39) along the domain $0 \leq s \leq L_b$. The largest value occurs at $s = L_b$, see Figure 3d:

$$u_{i,max} = \frac{u_b}{L_b} \left[\frac{\zeta^2 L_b \sinh(\zeta L_b)}{\beta_c \zeta L_b \cosh(\zeta L_b) + \beta_s \sinh(\zeta L_b)} \right] \tag{44}$$

Equations 42, 43 and 44 show that the maximum strains — and therefore the maximum stresses — in the segment vary with segment length L_b and segment elongation u_b.

At the location of cortex failure ($s = L_b$) the stele carries the entire tensile force T_r (Figure 3a), so the tensile force applied to the root can be expressed in terms of the stele response at the location of cortex failure as:

$$T_r = E_s A_s \epsilon_{s,max} \tag{45}$$

The tensile force T_r (and therefore $\epsilon_{s,max}$) has to be equal in each segment. The total root elongation is equal to the sum of elongations in all segments:

$$u_r = \epsilon_r L_r = \sum u_b \tag{46}$$

so with known segment lenghts L_b, a relationship between root tensile force T_r and root strain ϵ_r can be established by combining Equations 42, 45 and 46:

$$\epsilon_r = \frac{T_r}{E_s A_s L_r} \sum \frac{\beta_c \zeta L_b \cosh(\zeta L_b) + \beta_s \sinh(\zeta L_b)}{\zeta^3 \cosh(\zeta L_b)} \tag{47}$$

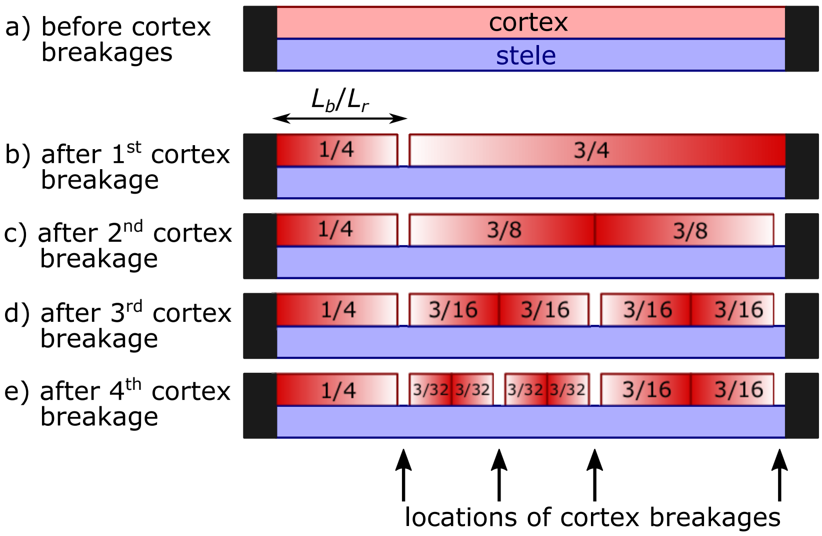

Figure 4: Schematic representation of the relationship between root segment lenghts and locations of cortex breakages. The white end of each cortex segment indicates where the cortex is broken, while the (darker) red end indicates where $u_c = u_s$ (at either clamp, or halfway neighbouring cortex breakages because of symmetry considerations.

8.2 Cortex failure as a discrete process

Continue to assume that the root interface remains fully intact during root tensioning. Immediately after root yielding, the cortex is broken at a single point along the root, for example at $s = L_r/4$ (but could be anywhere, depending in a local weakness in the cortex), resulting in two root segments with lengths $L_r/4$ and $3L_r/4$, see Figure 4b. Given the current level of root strain ϵ_r, the root force T_r can be calculated using Equation 47.

Just after the cortex breakage the stresses in the stele and cortex will reduce slightly since the root is now damaged. However, with increased levels of root strain ϵ_r stele and cortex stresses will increase again, until the cortex breaks again. This breakage will always occur at the largest distance from any existing breakage (as this is where stresses in the cortex will be largest, see Section 8.1). In our example, the second cortex breakage will occur at $s = L_r$, see Figure 4c.

The root is now separated into an increased number of segments (with lengths $L_r/4$, $3L_r/8$ and $3L_r/8$ in our example, see Figure 4c), for which the strains and stresses can be calculated again etc. In our example, the next cortex breakage will occur at $s = 5L_r/8$, resulting in segment lengths $L_r/4$, $3L_r/16$, $3L_r/16$, $3L_r/16$ and $3L_r/16$, see Figure 4d. This process of continuing discrete cortex failure will continue until eventually the strength in the stele is exceeded and the stele breaks, resulting in a fully broken root.

This process of ongoing cortex breakage and its effect on the root stress–strain behaviour is graphically demonstrated in Figure 5. This figure shows that the process of subsequent cortex failures results in a reduction of the root stiffness beyond the yield point. The stress–strain response shows 'sawtooth'-like behaviour, in which each sudden reduction in root stress corresponds to an individual cortex breakage event.

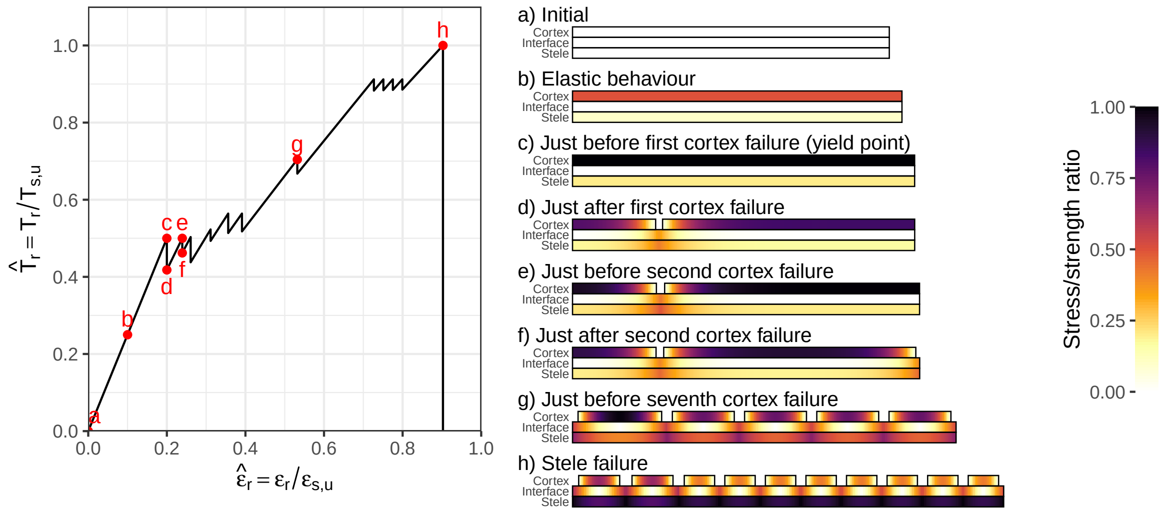

Figure 5: Stress–strain response of a root experiencing subsequent discrete breakages of the cortex. Subplots a) to h) show the stresses in the cortex, stele and interface (nondimensionalised by their respective strengths) along the stretched root axis at different points during the test indicated by letters a–h in the left-most plot.

8.3 Cortex failure as a continuous process

Rather than describing this process of cortex failure as a discrete set of cortex failures in which the segment lengths L_b reduce *step-wise*, this process can be modelled as a 'continuous' cortex breakage process in which the segment length L_b reduces *gradually and continuously*. This enables deriving a single analytical expression for this part of the stress–strain curve.

In the case of continuous cortex failure, $\epsilon_{c,max} = \epsilon_{c,u}$ after reaching the yield point, i.e. the cortex will be continuously breaking somewhere along the root. Dividing Equation 42 by Equation 43 and substituting $\epsilon_{c,max} = \epsilon_{c,u}$ gives:

$$\frac{\epsilon_{s,max}}{\epsilon_{c,max}} = \frac{\epsilon_{s,max}}{\epsilon_{c,u}} = \frac{\zeta^2 \cosh\left(\zeta L_b\right)}{\beta_c(\cosh\left(\zeta L_b\right) - 1)} \tag{48}$$

Solving this for segment length L_b gives:

$$L_b = \frac{1}{\zeta} \cosh^{-1}\left(\frac{\beta_c \epsilon_{s,max}}{\beta_c \epsilon_{s,max} - \zeta^2 \epsilon_{c,u}}\right) \tag{49}$$

Now substitute this expression for L_b (Equation 49) into Equation 42 to find an expression for root strain $\epsilon_r = u_b/L_b$ as function of maximum stele stress $\epsilon_{s,max}$:

$$\epsilon_r = \frac{u_b}{L_b} = \frac{\epsilon_{s,max}}{\zeta^2}\left[\beta_c + \frac{\beta_s\sqrt{1-\left(\frac{\beta_c\epsilon_{s,max}-\zeta^2\epsilon_{c,u}}{\beta_c\epsilon_{s,max}}\right)^2}}{\cosh^{-1}\left(\frac{\beta_c\epsilon_{s,max}}{\beta_c\epsilon_{s,max}-\zeta^2\epsilon_{c,u}}\right)}\right] \tag{50}$$

Substituting the relationship between maximum stele stress $\epsilon_{s,max}$ and root tensile force T_r (Equation 45) gives the stress–strain relationship for the root in case of continuous cortex breakage:

$$\epsilon_r = \frac{T_r}{E_s A_s \zeta^2}\left[\beta_c + \frac{\beta_s\sqrt{1-\left(\frac{\beta_c T_r - E_s A_s \zeta^2 \epsilon_{c,u}}{\beta_c T_r}\right)^2}}{\cosh^{-1}\left(\frac{\beta_c T_r}{\beta_c T_r - E_s A_s \zeta^2 \epsilon_{c,u}}\right)}\right] \tag{51}$$

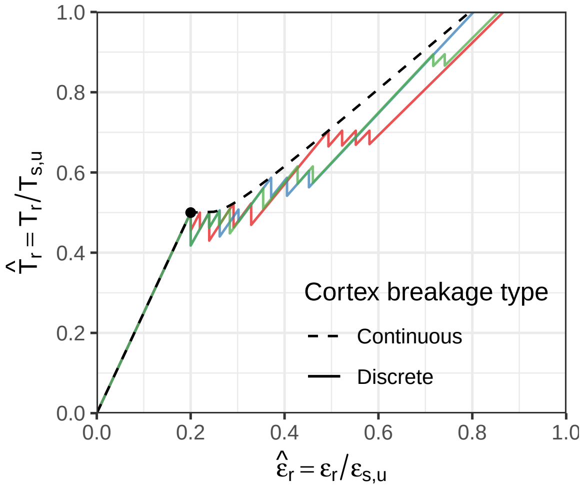

Figure 6: Stress–strain response for continuous (dashed) versus discrete cortex failure (solid lines). Colours represent different assumptions for the location of the initial discrete cortex failure. The black dot indicates the position of the yield point, associated with the initial failure in the cortex.

Subsequent substitutions of ζ, β_s and β_c using Equations 23, 24 and 25 respectively gives:

$$\epsilon_r = \frac{T_r}{E_s A_s + E_c A_c} \left[1 + \frac{\sqrt{1 - \left(\frac{T_r - (E_s A_s + E_c A_c)\epsilon_{c,u}}{T_r} \right)^2}}{E_s A_s \cosh^{-1} \left(\frac{T_r}{T_r - (E_s A_s + E_c A_c)\epsilon_{c,u}} \right)} \right] \tag{52}$$

Using the expression for the yield force $T_{r,y} = (E_s A_s + E_c A_c)\epsilon_{c,u}$ (Equation 18), this can be written as:

$$\epsilon_r = \epsilon_{c,u} \left[\frac{T_r}{T_{r,y}} + \frac{E_c A_c \sqrt{\frac{2T_r}{T_{r,y}} - 1}}{E_s A_s \cosh^{-1} \left(\frac{T_r}{T_r - T_{r,y}} \right)} \right] \tag{53}$$

Further substituting using expressions for $T_{s,u}$ and $T_{c,u}$ (Equations 1 and 2) gives:

$$\epsilon_r = \frac{T_r \epsilon_{c,u}}{T_{r,y}} + \frac{T_{c,u} \epsilon_{s,u} \sqrt{\frac{2T_r}{T_{r,y}} - 1}}{T_{s,u} \cosh^{-1} \left(\frac{T_r}{T_r - T_{r,y}} \right)} \tag{54}$$

This continuous solution for root tensile force T_r as function of root strain ϵ_r forms the upper bound for all discrete cortex breakage mechanisms with different positions of initial cortex failures, see Figure 6. Using a continuous rather than discrete cortex failure is much more convenient as the root response can now be expressed using a single analytical expression (Equation 53), rather than the iterative process described in Section 8.2, while still conserving the correct underlying mechanics.

8.4 Stele–cortex interface debonding

After initial cortex failure ($\epsilon_r > \epsilon_{r,y}$), interface resistance between stele and cortex will start to develop (see Equation 44 and also Figure 5). So far, it was assumed that the interface strength is never exceeded and the cortex–stele interface will never debond. Let us now consider what happens when the stele–cortex debonding may occur.

Debonding will occur once $u_{i,max} = u_{i,u}$. Assuming continuous cortex breakage (so $\epsilon_{c,max} = \epsilon_{c,u}$), substituting Equation 43 into Equation 44 shows interface debonding will commence once cortex segment length L_b has been reduced to a value $L_{b,u}$:

$$L_{b,u} = \frac{2}{\zeta} \tanh^{-1} \left(\frac{\zeta \epsilon_{c,u}}{\beta_c u_{i,u}} \right) \tag{55}$$

The corresponding value of $\epsilon_{s,max}$ can be found by dividing Equation 44 by Equation 42:

$$\frac{u_{i,max}}{\epsilon_{s,max}} = \frac{\zeta^2 L_b \sinh(\zeta L_b)}{\zeta^3 L_b \cosh(\zeta L_b)} = \frac{1}{\zeta} \tanh(\zeta L_b) \tag{56}$$

After substituting $u_{i,max} = u_{i,u}$ and $L_b = L_{b,u}$ into Equation 56 and subsequent reordering of terms, the maximum stele strain at which debonding commences can be written as:

$$\epsilon_{s,max} = \frac{\zeta u_{i,u}}{\tanh(\zeta L_{b,u})} = \frac{\beta_c u_{i,u}^2}{2\epsilon_{c,u}} + \frac{\zeta^2 \epsilon_{c,u}}{2\beta_c} \tag{57}$$

The tensile force T_r at which debonding commences is therefore given by:

$$T_r = E_s A_s \epsilon_{s,max} = \frac{E_s A_s \beta_c u_{i,u}^2}{2\epsilon_{c,u}} + \frac{E_s A_s \zeta^2 \epsilon_{c,u}}{2\beta_c} \tag{58}$$

Once the interface starts to debond the cortex will cease to break (debonding is now the critical failure mechanism rather than cortex failure). The length of cortex segments will from now on remain constant with increasing applied tensile force T_r (segment length $L_b = L_{b,u}$) but the cortex and stele will instead start to debond, starting from the point where the cortex is broken (Figure 7a).

Assume the cortex and stele will remain bonded over a length L_b and debond over a length $L_d = L_{b,u} - L_b$ (Figure 7b). At the location where the interface debonds ($s = L_b$):

$$u_i = u_{i,u} \tag{59}$$

Across the debonded part of the root, the stele and cortex are no longer connected and therefore cannot transfer any forces (i.e. $T_i = 0$, Figure 7c). Thus the tensile forces will be constant across these sections (Equation 12), and therefore the stresses and strains will also be constant:

$$\epsilon_s(s > L_b) = \epsilon_{s,max} \tag{60}$$

$$\epsilon_c(s > L_b) = 0 \tag{61}$$

The (average) root strain ϵ_r along the segment is determined using summation of the elongations in the bonded and debonded parts of the segment (Figure 7d):

$$L_{b,u}\epsilon_r = u_b + (L_{b,u} - L_b)\epsilon_{s,max} \tag{62}$$

where u_b is the stele elongation in the bonded part of the segment, and $(L_{b,u} - L_b)\epsilon_{s,max}$ the stele elongation along the debonded part of the segment.

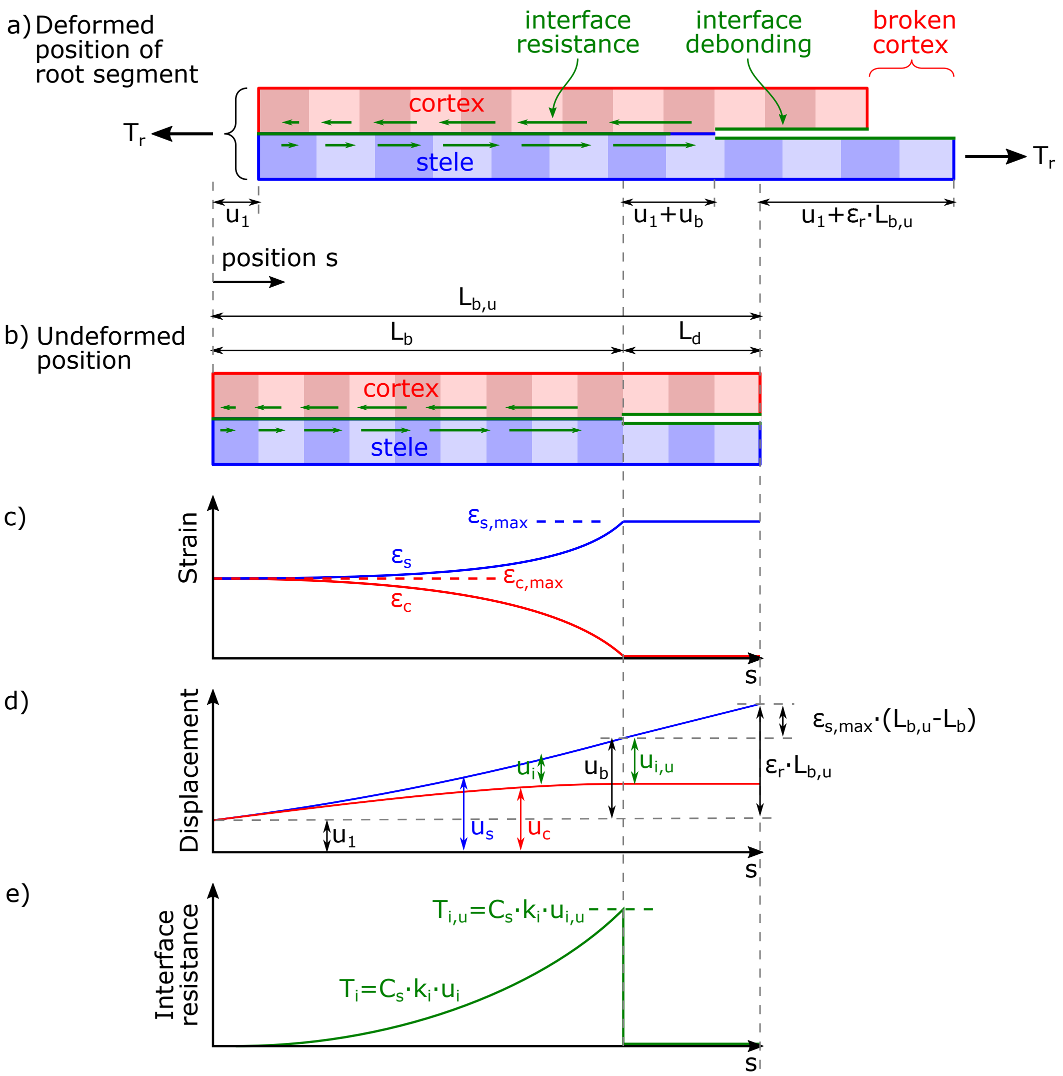

Figure 7: Schematic of root strains and displacements along the root axis of a (partially) debonding segment of root

This system of equations can again be solved analytically in order to obtain root strain ϵ_r as function of root force T_r. First obtain the bonded length L_b by dividing Equations 44 by Equation 42.

$$\frac{u_{i,max}}{\epsilon_{s,max}} = \frac{u_{i,u}}{\epsilon_{s,max}} = \frac{1}{\zeta}\tanh\left(\zeta L_b\right) \tag{63}$$

Solving for L_b gives:

$$L_b = \frac{1}{\zeta}\tanh^{-1}\left(\frac{\zeta u_{i,u}}{\epsilon_{s,max}}\right) \tag{64}$$

Now find u_b by substituting L_b into Equation 44 and using $u_{i,max} = u_{i,u}$:

$$u_b = \frac{\beta_c \epsilon_{s,max}}{\zeta^3}\tanh^{-1}\left(\frac{\zeta u_{i,u}}{\epsilon_{s,max}}\right) + \frac{\beta_s u_{i,u}}{\zeta^2} \tag{65}$$

Substitute Equations 55, 64 and 65 into Equation 62 to obtain ϵ_r:

$$\epsilon_r = \epsilon_{s,max} + \frac{\beta_s \zeta u_{i,u} - \beta_s \epsilon_{s,max}\tanh^{-1}\left(\frac{\zeta u_{i,u}}{\epsilon_{s,max}}\right)}{2\zeta^2 \tanh^{-1}\left(\frac{\zeta \epsilon_{c,u}}{\beta_c u_{i,u}}\right)} \tag{66}$$

Substituting the relationship between maximum stele stress $\epsilon_{s,max}$ and root tensile force $T_r = E_s A_s \epsilon_{s,max}$ (Equation 45) gives the stress–strain relationship for the interface debonding behaviour:

$$\epsilon_r = \frac{T_r}{E_s A_s} + \frac{\beta_s \zeta u_{i,u} - \frac{\beta_s T_r}{E_s A_s}\tanh^{-1}\left(\frac{\zeta u_{i,u} E_s A_s}{T_r}\right)}{2\zeta^2 \tanh^{-1}\left(\frac{\zeta \epsilon_{c,u}}{\beta_c u_{i,u}}\right)} \tag{67}$$

After substituting expressions for ζ, β_s and β_c (Equation 23, 24 and 25 respectively) and multiplying both the numerator and denominator of the second fractional term by $E_s A_s E_c A_c$:

$$\epsilon_r = \frac{T_r}{E_s A_s} + \frac{u_{i,u}\sqrt{E_s A_s E_c A_c (E_s A_s + E_c A_c) C_s k_i} - T_r E_c A_c \tanh^{-1}\left(\frac{u_{i,u}}{T_r}\sqrt{\frac{E_s A_s (E_s A_s + E_c A_c) C_s k_i}{E_c A_c}}\right)}{2 E_s A_s (E_s A_s + E_c A_c)\tanh^{-1}\left(\frac{\epsilon_{c,u}}{u_{i,u}}\sqrt{\frac{E_c A_c (E_s A_s + E_c A_c)}{E_s A_s C_i k_i}}\right)} \tag{68}$$

After substitution of expressions for $T_{s,u}$ (Equation 1), $T_{c,u}$ (Equation 2), $T_{i,u}$ (Equation 7) and $T_{r,y}$ (Equation 18):

$$\epsilon_r = \frac{T_r \epsilon_{s,u}}{T_{s,u}} + \frac{\sqrt{T_{s,u} T_{c,u} T_{r,y} T_{i,u} u_{i,u} \epsilon_{s,u}} - T_r T_{c,u}\epsilon_{s,u}\tanh^{-1}\left(\sqrt{\frac{T_{s,u} T_{r,y} T_{i,u} u_{i,u}}{T_r^2 T_{c,u} \epsilon_{s,u}}}\right)}{2 T_{s,u} T_{r,y}\tanh^{-1}\left(\sqrt{\frac{T_{c,u} T_{r,y} \epsilon_{s,u}}{T_{s,u} T_{i,u} u_{i,u}}}\right)} \tag{69}$$

9 Nondimensionalised solutions

9.1 Nondimensional parameter groups

It is convenient to express stress–strain solutions found above using nondimensional parameter groups. Forces are normalised by the force required to break the stele ($T_{s,u}$), while strains are normalised by the strain required to break the stele ($\epsilon_{s,u}$).

The nondimensional stress and strain parameters are defined as:

$$\hat{T}_r = \frac{T_r}{T_{s,u}} = \frac{A_r t_r}{A_s t_{s,u}} \tag{70}$$

$$\hat{\epsilon}_r = \frac{\epsilon_r}{\epsilon_{s,u}} \tag{71}$$

The entire problem can be expressed as a function of three dimensionless parameter groups:

- **Strength parameter** r_T describes the ratio between the cortex and stele strengths (in terms of forces):
$$r_T = \frac{T_{c,u}}{T_{s,u}} = \frac{A_c t_{c,u}}{A_s t_{s,u}} = \frac{E_c A_c \epsilon_{c,u}}{E_s A_s \epsilon_{s,u}} \tag{72}$$

- **Strain parameter** r_ϵ describes the ratio between the cortex and stele tensile strains to failure:
$$r_\epsilon = \frac{\epsilon_{c,u}}{\epsilon_{s,u}} \tag{73}$$

- **Interface parameter** r_i describes the strain energy (or mechanical work W) required to break the interface along the entire root length relative to the strain energy required to break the stele:
$$r_i = \frac{W_i}{W_s} = \frac{0.5 C_s L_r t_{i,u} u_{i,u}}{0.5 A_s L_r t_{s,u} \epsilon_{s,u}} = \frac{C_s t_{i,u} u_{i,u}}{A_s t_{s,u} \epsilon_{s,u}} = \frac{T_{i,u} u_{i,u}}{T_{s,u} \epsilon_{s,u}} \tag{74}$$

9.2 Dimensionless stress–strain equations

The previously derived solutions describing the full tensile stress–strain behaviour of any root, consisting of elastic, cortex failure and interface debonding parts, can be written in terms of the nondimensional parameter groups (Equations 70–74) defined in the previous section:

1. **Elastic behaviour** (see Section 6): This is the initial part of the curve where both the cortex and stele are fully intact. Rewriting Equation 17 using nondimensional parameter groups:
$$\hat{\epsilon}_r = \frac{r_\epsilon \hat{T}_r}{r_T + r_\epsilon} \tag{75}$$
This solution is valid when the yield strength has not been exceeded. In terms of nondimensional parameter groups:
$$\hat{T}_r \leq \hat{T}_{r,y} \tag{76}$$
where the (nondimensional) yield force $\hat{T}_{r,y} = T_{r,y}/T_{s,u}$ is found by rewriting Equation 18 in terms of nondimensional parameter groups:
$$\hat{T}_{r,y} = r_T + r_\epsilon \tag{77}$$

2. **Plastic hardening behaviour - (continuous) cortex breakage** (see Section 8.3): At the yield point the cortex will break. For the stele to remain intact after this initial cortex failure, Equation 19 — rewritten using nondimensional parameter groups — must hold:
$$r_T + r_\epsilon \leq 1 \tag{78}$$
If this condition is met, the root will be able to mobilise more stress after yielding, i.e. show hardening behaviour. The stress–strain behaviour during the subsequent phase of

continuous cortex breakage (Equation 54) can be written in terms of nondimensional parameter groups:

$$\hat{\epsilon}_r = \frac{r_\epsilon \hat{T}_r}{r_T + r_\epsilon} + \frac{r_T\sqrt{2\hat{T}_r - r_T - r_\epsilon}}{\sqrt{r_T + r_\epsilon}\cosh^{-1}\left(\frac{\hat{T}_r}{\hat{T}_r - r_T - r_\epsilon}\right)} \tag{79}$$

This solution is valid when the following conditions are met: a) the tensile force exceeds the yield force ($T_r > T_{r,y}$); b) the tensile force does not exceeds the force required to commence interface debonding (Equation 58); c) the tensile force is smaller than the force required to break the stele ($T_r \leq T_{s,u}$). Written in terms of non-dimensional parameter groups:

$$\hat{T}_r > r_T + r_\epsilon \quad \& \quad \hat{T}_r \leq \frac{1}{2}\left(\frac{r_i}{r_T} + r_T + r_\epsilon\right) \quad \& \quad \hat{T}_r \leq 1 \tag{80}$$

3. **Plastic hardening behaviour - interface debonding** (see Section 8.4): The stele and cortex will start to (partially) debond when the stresses in the stele–cortex interface exceed the interface strength. Rewriting this part of the root stress–strain curve (Equation 69) in terms of nondimensional parameter groups gives:

$$\hat{\epsilon}_r = \hat{T}_r + \frac{\sqrt{r_i r_T (r_T + r_\epsilon)} - r_T \tanh^{-1}\left(\frac{\sqrt{r_i r_T (r_\epsilon + r_T)}}{r_T \hat{T}_r}\right)\hat{T}_r}{2(r_T + r_\epsilon)\tanh^{-1}\left(\frac{r_T(r_T + r_\epsilon)}{\sqrt{r_i r_T (r_T + r_\epsilon)}}\right)} \tag{81}$$

This solution is valid when: a) the tensile force exceeds the yield force ($T_r > T_{r,y}$); b) the tensile force exceeds the force required to commence interface debonding (Equation 58); and c) the tensile force is smaller than the force required to break the stele ($T_r \leq T_{s,u}$). Written in terms of non-dimensional parameter groups:

$$\hat{T}_r > r_T + r_\epsilon \quad \& \quad \hat{T}_r > \frac{1}{2}\left(\frac{r_i}{r_T} + r_T + r_\epsilon\right) \quad \& \quad \hat{T}_r \leq 1 \tag{82}$$

The interface will remain intact and not debond during any part of the tensile test when the force required for interface debonding to commence (Equation 58) is larger than the force required to break the stele. In this case, the root will have failed in tension before any debonding may occur. Written in terms of nondimensional parameter groups, debonding will not occur when:

$$r_i \geq r_T(2 - r_T - r_\epsilon) \tag{83}$$

Together, Equations 75, 79 and 81 can describe the theoretical stress–strain behaviour of any root. An example curve is shown in Figure 8 for $r_T = 0.3$, $r_\epsilon = 0.2$ and various values of r_i.

10 Fitting of tensile stress–strain curves and determination of the yield point

Measured tensile stress–strain data must be analysed in order to extract information about the ultimate strength ($t_{r,u}$) and strain to peak ($\epsilon_{r,u}$), the yield point (yield stress $t_{r,y}$, yield strain $\epsilon_{r,y}$) and the effect of root tortuosity on these strains ($u_{r,t}$). The root behaviour in tension was assumed to consist of three different phases:

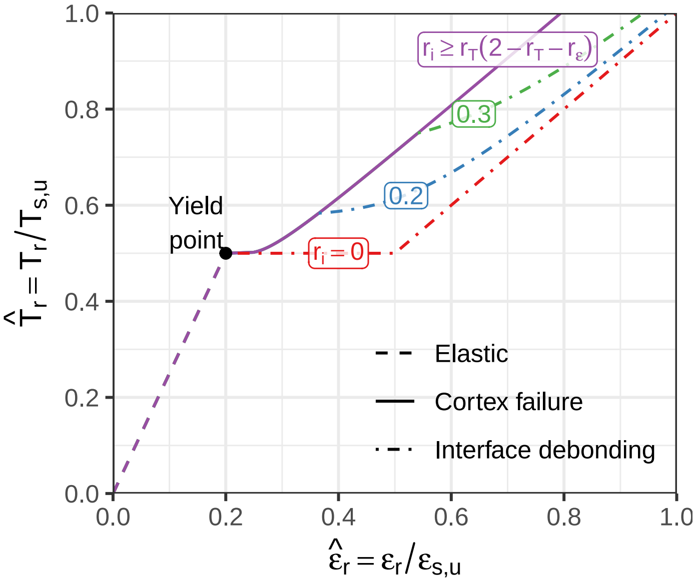

Figure 8: Example nondimensionalised stress–strain curves for $r_T = 0.3$, $r_\epsilon = 0.2$ and various values of r_i ranging from negligible interface strength ($r_i = 0$) to being strong enough so no debonding takes place during the tensile test ($r_i \geq r_T(2 - r_T - r_\epsilon)$).

1. Initial phase; associated with the stretching of a tortuous root. The stiffness is typically lower than the elastic root stiffness (Young's modulus)

2. Elastic phase, during which the stiffness is equal to the elastic root stiffness (Young's modulus)

3. Plastic phase, associated with a reduction in stiffness after root yield

The measured tensile force T_r versus displacement u_r curve was fitted with three corresponding linear segments using the following step-wise procedure:

1. Determine the tensile force ($T_{r,u}$) and displacement ($u_{r,u}$) at the ultimate point (maximum tensile force).

2. Smooth the measured force–displacement data to eliminate noise. The existence of noise will greatly affect numerical differentiation required to obtain gradients. A cubic smoothing spline was used (R function `smooth.spline()`, using a smoothing coefficient spar $= 0.75$).

3. Determine the point where the force–displacement gradient is largest (force $T_{r,e}$, displacement $u_{r,e}$, gradient G_e). This gradient is directly associated with the Young's modulus of the root.

4. Determine the plastic force–displacement gradient as the smallest possible gradient (G_p) of a line that passes through the ultimate point ($u_{r,u}$, $T_{r,u}$) and any measured point located between:

$$u_{r,e} \leq u_r \leq u_{r,e} + (1 - f)\,\frac{T_{r,u} - T_{r,e}}{G_e} + f\,(u_{r,u} - u_{r,e}) \tag{84}$$

When $f = 0$, the search is conducted between $u_{r,e}$ and the displacement required to break the root if the root were to behave purely elastic ($u_{r,e} + (T_{r,u} - T_{r,e})/G_e$). f can therefore be interpreted as the fraction of plastic root deformation to additionally include in the displacement search domain for determining the plastic stiffness ($0 \leq f \leq 1$). $f = 1/3$ was selected as this yielded good approximations of the plastic part of the curve, see Figures 9 and 10.

5. Determine the yield displacement $u_{r,y}$ and yield force $T_{r,y}$ as the intersection of the elastic and plastic gradient lines.

6. Determine the force, displacement and gradient at the start of the test ($T_{r,i}$, $u_{r,i}$, G_i). The displacement of the unstressed root at the start of the test ($u_{r,0}$, defined as the displacement at which $T_r = 0$) can be estimated by linear extrapolation if required:

$$u_{r,0} = u_{r,i} - \frac{T_{r,i}}{G_i} \tag{85}$$

If $u_{r,0} < 0$, the root is pre-streched during installation in the tensile test machine (resulting in some tensile force at zero displacement). Equally, if $u_{r,0} > 0$ the root is pre-compressed.

7. Calculate the estimated difference between arc length and span length ($u_{r,t} = L_r - L_s$) as:

$$u_{r,t} = u_{r,e} - \frac{T_{r,e}}{G_e} - u_{r,0} \tag{86}$$

8. Calculate the ultimate tensile strength and strain as:

$$t_{r,u} = \frac{T_{r,u}}{A_r} \tag{87}$$

$$\epsilon_{r,u} = \frac{u_{r,u} - u_{r,t}}{L_s + u_{r,t}} \tag{88}$$

9. Calculate the yield strength and strain as:

$$t_{r,y} = \frac{T_{r,y}}{A_r} \tag{89}$$

$$\epsilon_{r,y} = \frac{u_{r,y} - u_{r,t}}{L_s + u_{r,t}} \tag{90}$$

A graphical example of this fitting procedure for root tensile test 578 is shown in Figure 9.

Figure 10 shows both the measured and fitted force–displacement curves for all successful tensile tests conducted. This demonstrated the adopted multi-linear fitting approach approximated the measured data well.

11 Symbols

All parameters in this manuscript, unless otherwise specified, are expressed in generic dimensions: [F] for units of force, [L] for units of length/diameter and [-] for dimensionless parameters. This allows the reader to use their own preferred set of units in each equation.

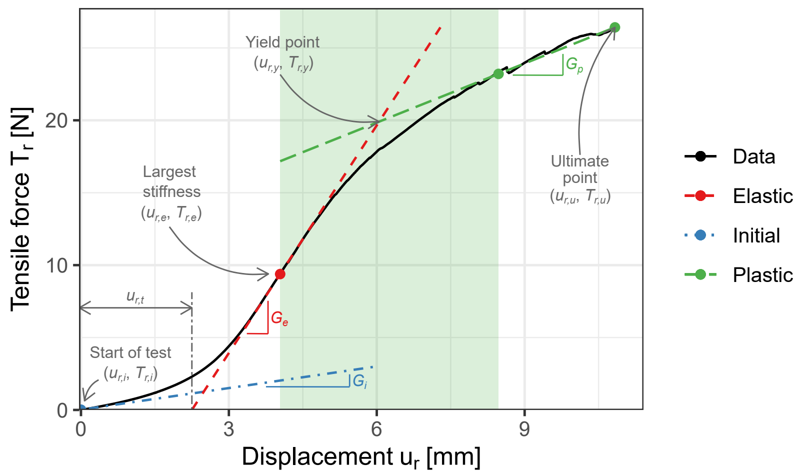

Figure 9: Schematic showing the method of fitting force–displacement data and determination of the yield point. The light green shaded zone indicates the search window for finding the plastic stiffness. Data for root sample 578 was used. f was chosen as 1/3.

11.1 Parameter and subscript logic

The symbols for commonly used parameters follow the following logic:

- ϵ: Strain [LL^{-1}]
- A: Cross-sectional area [L^2]
- C: Circumference [L]
- E: Young's modulus [FL^{-2}]
- k: Spring stiffness [FL^{-3}]
- L: Length [L]
- s: Positional coordinate [L]
- T: Tensile force [F]
- t: Tensile stress [FL^{-2}]
- u: Displacement [L]
- W: Mechanical work, or strain energy [FL]

Subscripts follow the following logic:

- $\square_c$: Cortex
- $\square_i$: Stele–cortex interface
- $\square_{max}$: Maximum value along a segment
- $\square_r$: Root
- $\square_s$: Stele
- $\square_u$: Value at failure

Subscripts may be combined, i.e. $t_{s,u}$, which is the symbol used for stele tensile strength, is the *tensile stress* (t) in the *stele* (subscript s) at the moment of *failure* (subscript u).

Other notations commonly used are:

- $\hat{\square}$: Nondimensionalised parameter $\square$
- $\bar{\square}$: Prediction for parameter $\square$

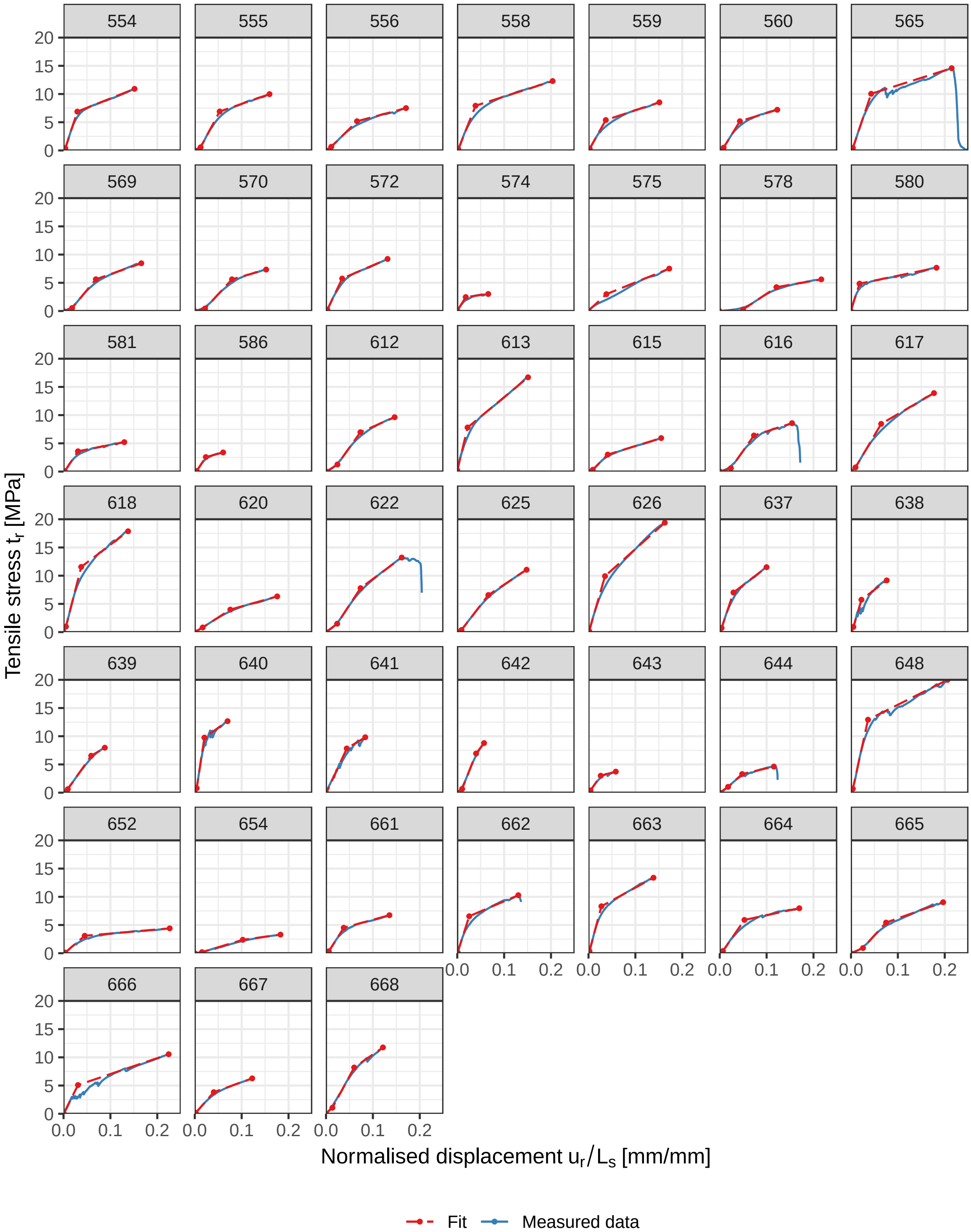

Figure 10: Measured and fitted tensile stress (t_r) versus displacement u_r (normalised by span length L_s) traces for all successful tensile tests. Each subfigure contains the data for one test.

11.2 Full list of symbols

A full list of all symbols used:

- ϵ_c: Current cortex tensile strain [LL^{-1}]
- $\epsilon_{c,max}$: Largest stress in the cortex along a root 'segment' [LL^{-1}]
- $\epsilon_{c,u}$: Cortex tensile strain at cortex failure [LL^{-1}]
- $\hat{\epsilon}_r$ Nondimensionalised root tensile strain [-]
- ϵ_r: (Average) root tensile strain [LL^{-1}]
- $\epsilon_{r,u}$: (Average) root tensile strain to peak [LL^{-1}]
- $\epsilon_{r,y}$: Root tensile yield strain [LL^{-1}]
- ϵ_s: Current stele tensile strain [LL^{-1}]
- $\epsilon_{s,max}$: Largest stress in the stele along a root 'segment' [LL^{-1}]
- $\epsilon_{s,u}$: Stele tensile strain at stele failure [LL^{-1}]
- A_c: Cross-sectional area of the cortex [L^2]
- A_r: Cross-sectional area of the root [L^2]
- A_s: Cross-sectional area of the stele [L^2]
- C_s: Circumreference of the stele [L]
- E_c: Young's modulus of the cortex [FL^{-2}]
- E_s: Young's modulus of the stele [FL^{-2}]
- k_i: Stele–cortex interface stiffness [FL^{-3}]
- L_r: Root length [L]
- L_b: Length of the part of root 'segment' along which the cortex–stele interface remains intact [L]
- $L_{b,u}$: Length of the root 'segment' at the onset of cortex–stele debonding [L]
- R^2: Coefficient of determination [-]
- r_ϵ: Nondimensionalised strain parameter [-]
- r_i: Nondimensionalised interface parameter [-]
- r_T: Nondimensionalised strength parameter [-]
- s: Coordinate along the root axis [L]
- T_c: Current tensile force in the cortex [F]
- $T_{c,u}$: Tensile force in cortex at cortex failure [F]
- $\hat{T}_r$ Nondimensionalised root tensile force [-]
- T_r: Current tensile force in the root [F]
- T_s: Current tensile force in the stele [F]
- $T_{s,u}$: Tensile force in stele at stele failure [F]
- t_c: Current cortex tensile stress [FL^{-2}]
- $t_{c,u}$: Cortex tensile strength [FL^{-2}]
- t_i: Current stele–cortex interface shear stress [FL^{-2}]
- $t_{i,u}$: Stele–cortex interface shear strength [FL^{-2}]
- t_r: Current root tensile stress [FL^{-2}]
- $t_{r,u}$: Root tensile strength [FL^{-2}]
- $t_{r,y}$: Root yield strength [FL^{-2}]
- t_s: Current stele tensile stress [FL^{-2}]

- $t_{s,u}$: Stele tensile strength [FL^{-2}]
- u_c: Axial displacement of a point along the cortex [L]
- u_i: Relative displacement between the stele and cortex [L]
- $u_{i,max}$: Maximum relative displacement between the stele and cortex along a root 'segment' [L]
- $u_{i,u}$: Relative displacement between the stele and cortex at which the stele–cortex interface debonds [L]
- u_r: Root elongation in tensile test [L]
- u_s: Axial displacement of a point along the stele [L]
- W_i: Work (energy) required to debond the entire stele–cortex interface [FL]
- W_s: Work (energy) required to break the stele [FL]

References

J. G. Chimungu, K. W. Loades, and J. P. Lynch. Root anatomical phenes predict root penetration ability and biomechanical properties in maize (Zea Mays). *Journal of Experimental Botany*, 66(11):3151–3162, 2015. doi: 10.1093/jxb/erv121.